



## Research article

# *Magnolia officinalis* Rehder & E. Wilson ameliorates white adipogenesis by upregulating AMPK and SIRT1 *in vitro* and *in vivo*

Yea-Jin Park<sup>a,b</sup>, Hee-Young Kim<sup>b</sup>, Tae-Young Gil<sup>b</sup>, Hyo-Jung Kim<sup>b</sup>, Jong-Sik Jin<sup>c</sup>, Yun-Yeop Cha<sup>a</sup>, Hyo-Jin An<sup>b,d,\*</sup><sup>a</sup> Department of Rehabilitative Medicine of Korean Medicine and Neuropsychiatry, College of Korean Medicine, Sangji University, Wonju, Gangwon-do, 26339, Republic of Korea<sup>b</sup> Department of Oriental Pharmaceutical Science, College of Pharmacy, Kyung Hee University, Seoul, 02447, Republic of Korea<sup>c</sup> Department of Oriental Medicine Resources, Jeonbuk National University, Iksan, 54596, Republic of Korea<sup>d</sup> Department of Integrated Drug Development and Natural Products, Graduate School, Kyung Hee University, Seoul, 02447, Republic of Korea

## ARTICLE INFO

## Keywords:

Magnolia cortex  
Obesity  
Adipose tissue  
Sirtuin 1  
AMP-Activated kinase

## ABSTRACT

Although there is an established link between Magnolia Cortex (MO) and lipid metabolism in previous research, its exploration within the context of obesity has been limited. Therefore, the present study investigated the therapeutic effects of MO on obesity and its mechanism of action *in vitro* and *in vivo*. Our chromatography analysis revealed that Honokiol and Magnolol are contained in MO extract. *In vitro* experiments showed that lipid droplets, adipogenic, and lipogenic genes were notably diminished by increasing sirtuin 1 (SIRT1) and AMP-activated kinase (AMPK) protein expression in MO-treated 3T3-L1 adipocytes. *In vivo* experiments exhibited that MO administration significantly recovered the adipogenesis, lipogenesis, and fatty acid oxidation genes by increasing the SIRT1 and AMPK expression in white adipose tissue. Furthermore, hepatic steatosis by HFD feeding was ameliorated in MO-administered obese mice. We conclude that MO could be important manager for treating obesity through AMPK and SIRT1 regulation.

## 1. Introduction

Obesity leads to a decreased life expectancy of up to ~20 years due to increased mortality from non-communicable diseases, e.g. atherosclerotic cardiovascular diseases, type 2 diabetes, and certain types of cancer [1]. Obesity is closely related to excessive accumulation of white adipose tissue, which mainly results from hyperplasia (adipocyte number increase) and hypertrophy (adipocyte size increase) [2]. When adipogenesis is occurred, peroxisome proliferator-activated receptor  $\gamma$  (PPAR $\gamma$ ) and CCAAT/enhancer-binding protein  $\alpha$  (C/EBP $\alpha$ ) are transactivated and they motivate lipogenesis-related factors that are essential for lipid formation and accumulation, such as sterol regulatory element-binding protein 1c (SREBP1c) [2]. Herein, the critical role for Sirtuin 1 (SIRT1), a NAD<sup>+</sup>-dependent deacetylase, in adipogenesis have been highlighted *in vitro* and *in vivo* studies [3]; therefore, it has also been suggested that pharmacological SIRT1 activation may prevent metabolic disorder related to obesity or other metabolic dysfunction [4].

*Magnolia officinalis* Rehder & E. Wilson is part of the Magnoliaceae family. Magnolia Cortex (MO) has been used to treat diverse

\* Corresponding author. Department of Oriental Pharmaceutical Science, College of Pharmacy, Kyung Hee University, Seoul, 02447, Republic of Korea.

E-mail addresses: [wer0928@hanmail.net](mailto:wer0928@hanmail.net) (Y.-J. Park), [heeyoung31@nate.com](mailto:heeyoung31@nate.com) (H.-Y. Kim), [sophia14t@gmail.com](mailto:sophia14t@gmail.com) (T.-Y. Gil), [hyojung\\_95@naver.com](mailto:hyojung_95@naver.com) (H.-J. Kim), [jongsik.jin@jbnu.ac.kr](mailto:jongsik.jin@jbnu.ac.kr) (J.-S. Jin), [omdcha@sangji.ac.kr](mailto:omdcha@sangji.ac.kr) (Y.-Y. Cha), [hjan@khu.ac.kr](mailto:hjan@khu.ac.kr) (H.-J. An).

<https://doi.org/10.1016/j.heliyon.2024.e27600>

Received 29 August 2023; Received in revised form 3 March 2024; Accepted 4 March 2024

Available online 7 March 2024

2405-8440/© 2024 The Authors. Published by Elsevier Ltd. This is an open access article under the CC BY-NC-ND license (<http://creativecommons.org/licenses/by-nc-nd/4.0/>).

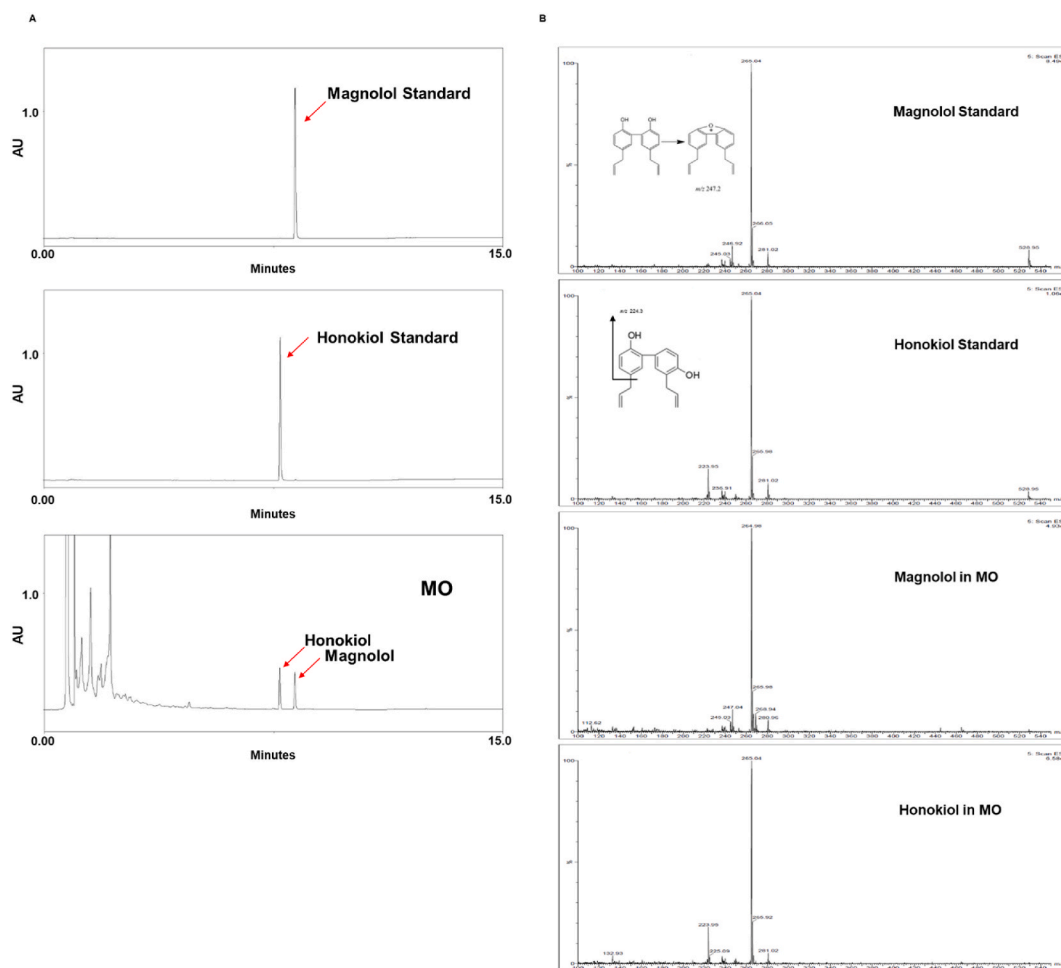


**Fig. 1.** Analysis of Magnolol and Honokiol in MO. UV chromatogram (A) and mass fragmentation pattern (B) of Magnolol, Honokiol, and MO.

conditions, such as abdominal distention, vomiting, food accumulation, Qi stagnation, phlegm, and fluid retention [5]. In addition, MO is traditionally used in gastrointestinal diseases, including digestive disorders, diarrhea, and constipation [6], which are well known risk factors of overweight and obesity [7]. The herbal preparations containing MO have been reported to possess diverse activities, such as antioxidant, anti-inflammatory/antibacterial, antithrombotic/anti-platelet, antiepileptic, smooth muscle relaxant, hypoglycaemic, anti-dyspeptic/prokinetic, and hepato-protective [8]. Although the regulatory effects of MO on gastrointestinal and metabolic disorders serves the possibility that MO might have anti-obesity activity, the pharmacological action of MO on obesity have not been elucidated.

Magnolol and Honokiol are major bioactive compounds of MO, and many studies have been reported that both of them were associated with SIRT1 on diverse diseases, including mitochondrial dysfunction, inflammation, oxidative stress, hyperglycemia and diabetic myocardial ischemia/reperfusion injury [9–12]. Hence, the aim of the present study was to investigate whether and how MO prevents obesity and whether it has impacts on the regulation of the SIRT1 in adipose tissue.

## 2. Results

### 2.1. Identification of magnolol and honokiol from MO by liquid chromatography-mass spectrometry analysis (LC/MS) analysis

Liquid chromatography-mass spectrometry analysis (LC/MS) revealed that Magnolol and Honokiol were detected in MO extract (Fig. 1A and B). The retention time of Magnolol and Honokiol were 8.3 and 7.8 min, respectively. Moreover, quantitative analysis of Magnolol and Honokiol by the UPLC/UV system revealed a concentration of 2.67 and 3.04 mg/g in the extract, respectively (Fig. 1A). MS spectrum of Magnolol standard showed quasi-molecular ion peaks at  $m/z$  265 [ $M - H$ ]<sup>-</sup> and 247 [ $M - H_2O$ ]<sup>-</sup>. MS spectrum of Honokiol standard showed quasi-molecular ion peaks at  $m/z$  265 [ $M - H$ ]<sup>-</sup> and 224 [ $M - C_3H_5$ ]<sup>-</sup>. Same quasi-molecular ion peaks at  $m/z$  265 [ $M - H$ ]<sup>-</sup> were observed in Magnolol standard and Honokiol standard. However, retention times and fragmentation patterns

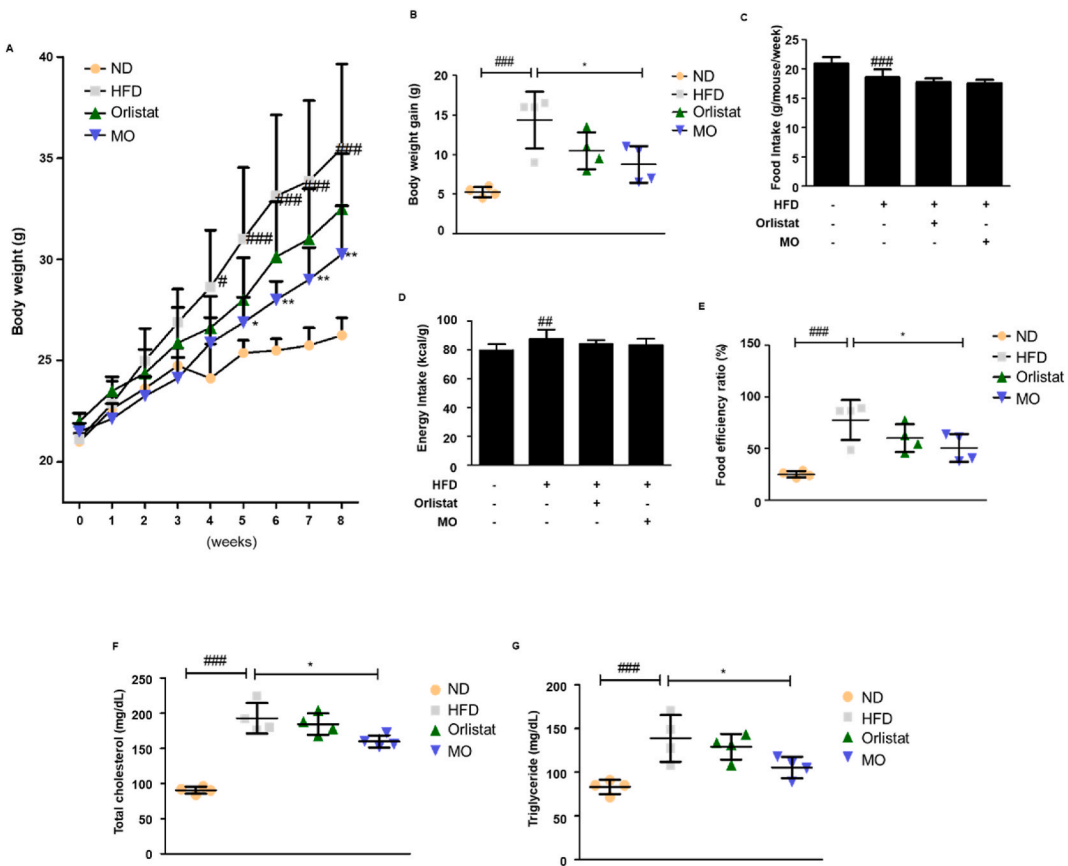


**Fig. 2.** Obesity is ameliorated in MO-administered mice. Male C57BL/6 mice were randomly assigned to the ND or the HFD group for 8 weeks. The HFD group was divided into three groups (n = 4 mice per group): HFD mice administered with water (vehicle), HFD mice administered with 20 mg/kg Orlistat, and HFD mice administered with 50 mg/kg MO. (A and C) Body weight and food intake were checked at 10 a.m. every Monday for 8 weeks. (B) Body weight gain. (C) Food intake. (D) Energy intake. (E) Food efficiency ratio. (F) Total cholesterol and (G) triglyceride levels were assessed. The values are represented as mean ± SD. #P < 0.05, ##P < 0.01, and ###P < 0.001 compared with ND group; \*P < 0.05 and \*\*P < 0.01 compared with HFD group; significances were determined using two-way ANOVA followed by a Bonferroni post hoc test, and one-way ANOVA followed by a Dunnett’s post hoc test.

were different (Fig. 1B).

**2.2. MO administration prevents the increased body weight gain, serum total cholesterol and triglyceride in vivo**

The high-fat diet (HFD)-fed mice showed increased body weight compared to the normal diet (ND)-fed mice, whereas MO administration significantly decreased the body weight gain from week 5 (Fig. 2A and B). MO administration did not change food and energy intake (Fig. 2C and D). However, the food efficiency ratio was significantly reduced after MO administration (Fig. 2E). The serum total cholesterol and triglyceride levels of HFD-fed group was higher than the ND-fed group, whereas MO-administered group improved these parameters of HFD-fed mice (Fig. 2F and G). No difference in these parameters was observed between HFD and Orlistat-administered groups (Fig. 2). In summary, these results showed that MO has protective effect against obesity in HFD-induced obese mice.

**2.3. White adipogenesis is attenuated via regulation of SIRT1/AMPK pathway in mice administered with MO**

To test if MO-administered mice exhibits altered adipose tissue characteristics, the weight and histological change in white adipose tissue were assessed. The white adipose tissue weights of HFD group were much larger compared to the Orlistat- and MO-administered groups (Fig. 3A). The HFD-fed mice had larger lipid droplets in white adipose tissue, which were markedly rescued by MO administration (Fig. 3B and C). To examine the mechanisms reducing white adipose tissue weights in MO-administered mice, the adipogenic-related proteins were assessed. The protein expression of PPARγ, SREBP1, and C/EBPα was higher in HFD-fed group but reversed by MO administration (Fig. 3D). In addition, MO administration significantly down-regulated the mRNA levels of lipogenic genes, fatty acid synthase (FAS) and carbohydrate response element-binding protein (ChREBP), and significantly up-regulated the mRNA levels of

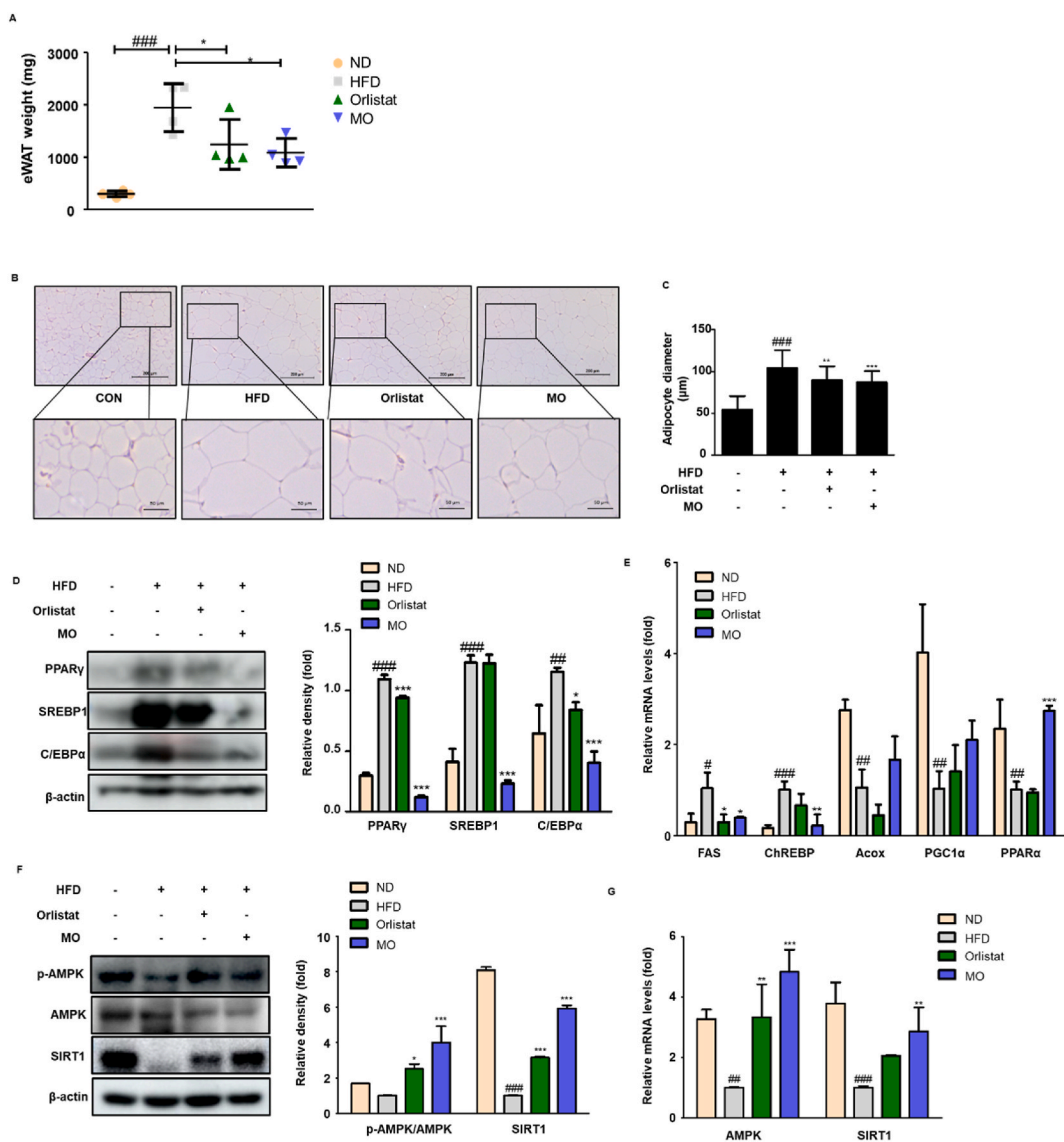


**Fig. 3.** Function of MO in the adipose tissue of HFD-fed obese mice.

(A) Epididymal white adipose tissue weight was measured at week 8 after Orlistat or MO administration. (B–C) H&E staining and adipocyte diameter in adipose tissue section. Scale bars are 200 (above) and 50 µm (below). (D) Western blot analysis of PPAR $\gamma$ , C/EBP $\alpha$ , and SREBP1 protein expression in adipose tissue. (E) qRT-PCR analysis of FAS, ChREBP, Acox, PGC-1 $\alpha$ , and PPAR $\alpha$  mRNA levels in adipose tissue. (F) Western blot of p-AMPK, AMPK, and SIRT1 protein expression in adipose tissue. Densitometric analysis was performed using ImageJ v1.50i. (G) qRT-PCR analysis of AMPK and SIRT1 mRNA levels in adipose tissue. The uncropped gel blots are provided as supplementary materials. The values are represented as mean  $\pm$  SD. #P < 0.05, ##P < 0.01, and ###P < 0.001 compared with ND group; \*P < 0.05, \*\*P < 0.01, and \*\*\*P < 0.001 compared with HFD group; significances were determined using one-way ANOVA followed by a Dunnett's post hoc test.

fatty acid oxidation gene PPAR $\alpha$ , with a shift towards increased acyl-CoA oxidase (Acox) and PPAR $\gamma$  coactivator 1 $\alpha$  (PGC1 $\alpha$ ) (Fig. 3E). Furthermore, it was notably up-regulated both of protein and mRNA expression of SIRT1 and AMP-activated kinase (AMPK) compared with HFD-fed group (Fig. 3F and G). Our results suggested that MO regulates white adipogenesis, lipogenesis, and fatty acid oxidation through activation of SIRT1/AMPK expression *in vivo*.

#### 2.4. MO inhibits adipocyte differentiation through the SIRT1/AMPK pathway *in vitro*

To evaluate whether MO has effects on cell viability in 3T3-L1 adipocytes, the cells were treated with concentrations of MO ranged from 0 to 1000 µg/mL. The cell viability was significantly suppressed by treatment with 250, 500, and 1000 µg/mL MO for 48 h, but lower concentration did not affect compared to the non-treated cells (Fig. 4A). To determine the effect of MO on adipocyte differentiation *in vitro*, we conducted Oil Red O staining in 3T3-L1 adipocyte. The differentiated cells exhibited increased lipid accumulation

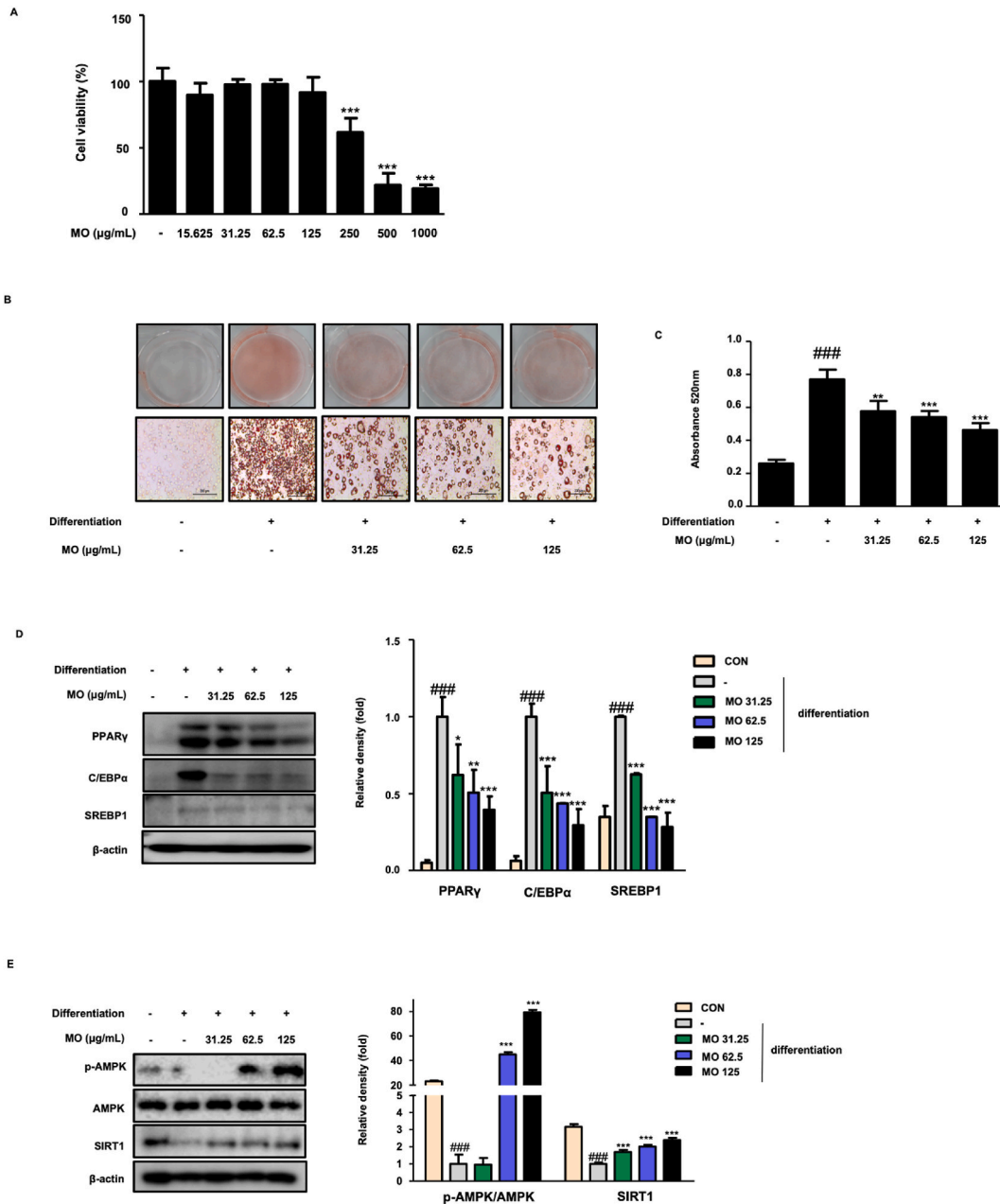


**Fig. 4.** Adipogenesis is lower in MO-treated 3T3-L1 adipocytes. (A) 3T3-L1 preadipocytes were incubated in culture medium with MO (0–1000 µg/mL) for 2 days. The cell viability was analyzed using MTT assay. \*\*\*P < 0.001 compared with untreated control. (B) 3T3-L1 preadipocytes were incubated in differentiation medium with MO (31.25–125 µg/mL) for 8 days. The lipid droplets were stained with Oil Red O. (C) The OD value of Oil Red O eluted solution. ###P < 0.001 vs. non-differentiation group; \*\*P < 0.01, and \*\*\*P < 0.001 compared with differentiation group. (D) 3T3-L1 preadipocytes were incubated in differentiation medium with MO (31.25–125 µg/mL) for 4 days, and then, cell lysates were collected and analyzed using western blotting with specific antibodies against PPARγ, C/EBPα, and SREBP1. (E) 3T3-L1 preadipocytes were incubated in MDI medium with MO for 2 h, and then, cell lysates were collected and analyzed using western blotting with specific antibodies against p-AMPK, AMPK, and SIRT1. β-actin was an internal control. Densitometric analysis was performed using ImageJ v1.50i. The uncropped gel blots are provided as supplementary materials. ###P < 0.001 vs. non-differentiation group; \*P < 0.05, \*\*P < 0.01, and \*\*\*P < 0.001 compared with differentiation group. The values are represented as mean ± SD and are representative of three independent experiments; significances were determined using one-way ANOVA followed by a Dunnett’s post hoc test. (For interpretation of the references to colour in this figure legend, the reader is referred to the Web version of this article.)

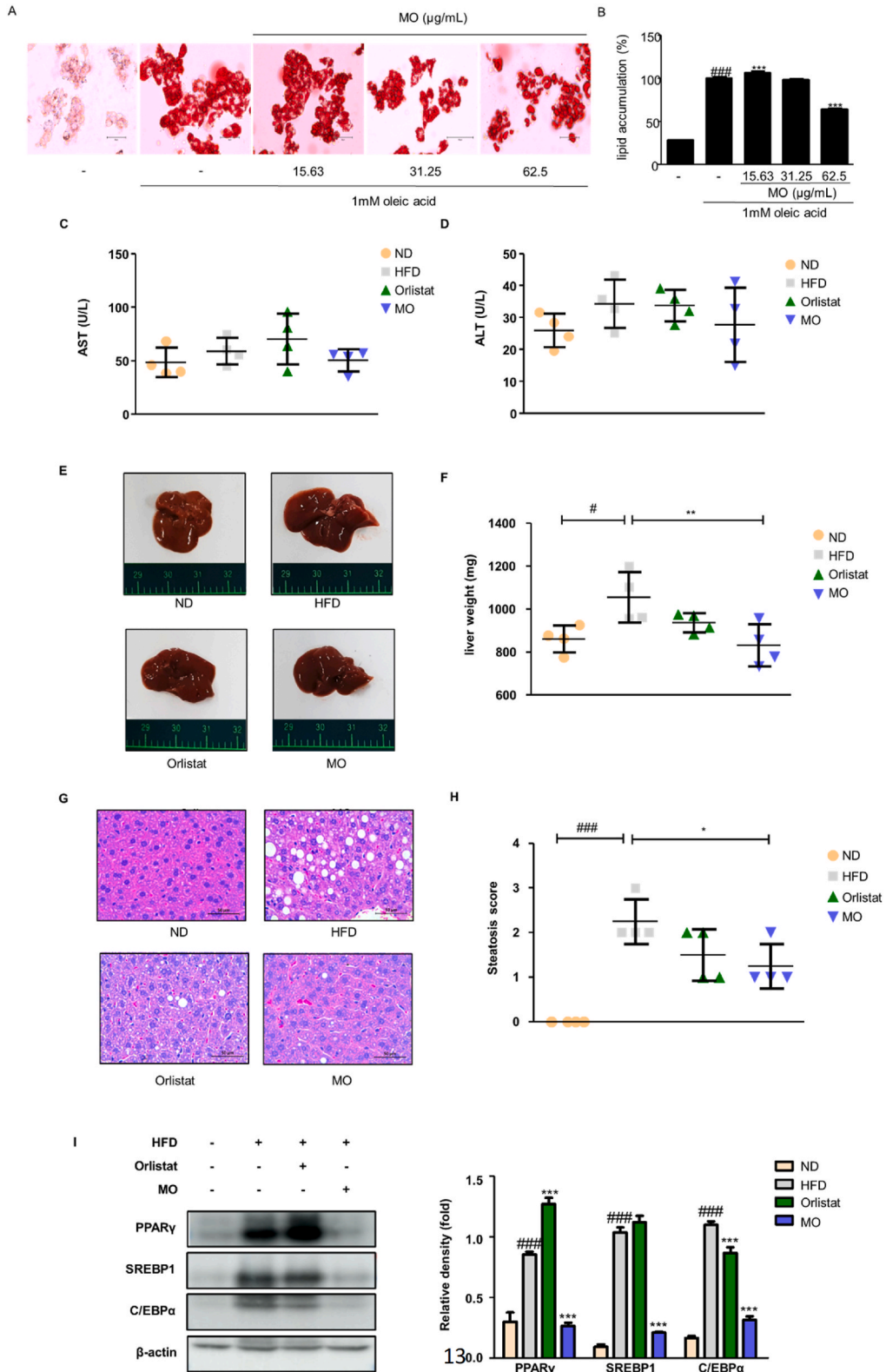


**Fig. 5.** MO administration improves hepatic steatosis *in vivo*

(A) Oleic acid was treated in HepG2 cells with or without MO (0–62.5 µg/mL) for 48 h. The lipid droplets were stained with Oil Red O. (B) The optical density value of Oil Red O eluted solution. ###P < 0.001 vs. non-cells; \*\*\*P < 0.001 compared with oleic acid-treated cells. (C) AST and (D)

ALT levels were assessed. (E) Representative images of liver. (F) The liver weight was measured at week 8 after Orlistat or MO administration. (G) H&E staining in liver section. (H) Steatosis score was measured using image J v1.50i. (I) Western blot analysis of PPAR $\gamma$ , C/EBP $\alpha$ , and SREBP1 protein expression in liver tissue. Densitometric analysis was performed using ImageJ v1.50i. The uncropped gel blots are provided as supplementary materials. The values are represented as mean  $\pm$  SD. <sup>#</sup>P < 0.05 and <sup>##</sup>P < 0.001 compared with ND group; \*P < 0.05, \*\*P < 0.01, and \*\*\*P < 0.001 compared with HFD group; significances were determined using one-way ANOVA followed by a Dunnett's post hoc test. (For interpretation of the references to colour in this figure legend, the reader is referred to the Web version of this article.)

compared to the non-treated cells, whereas MO treatment significantly decreased the lipid droplet in a dose-dependent manner (Fig. 4B and C). Moreover, we have analyzed the anti-adipogenic effects of MO and the two compounds in 3T3-L1 adipocytes. The lipid accumulation in MO-treated adipocytes significantly decreased, but not in Magnolol- and Honokiol-treated adipocytes (Fig. S1). The protein expression of PPAR $\gamma$  and C/EBP $\alpha$  which are adipogenic transcription factors, and SREBP1 which is lipogenic factors, was decreased after MO administration in differentiated 3T3-L1 adipocytes (Fig. 4D). Notably, MO treatment effectively up-regulated the protein expression of p-AMPK and SIRT1 in differentiated 3T3-L1 adipocytes (Fig. 4E).

### 2.5. Obesity-induced hepatic steatosis is ameliorated in MO-administered mice

To evaluate whether MO has effects on cell viability in HepG2 cells, the cells were treated with concentrations of MO ranged from 0 to 500  $\mu$ g/mL. The cell viability was significantly suppressed by treatment with 250 and 500  $\mu$ g/mL MO for 48 h, but lower concentration did not affect compared to the non-treated cells (Fig. S2). To assess the effect of MO on hepatic steatosis *in vitro*, we conducted Oil Red O staining in HepG2 cells. The oleic acid-treated cells exhibited increased lipid accumulation compared to the non-treated cells, whereas 62.5  $\mu$ g/mL MO treatment significantly decreased the lipid accumulation compared to the oleic-acid-treated cells (Fig. 5A and B). Next, to further determine the effect of MO on fat deposition in the liver, serum AST and ALT levels, and weight and histological change in the liver were assessed. There were no differences in the serum AST and ALT levels among all groups (Fig. 5C and D). However, we found that HFD-fed mice had larger liver size and weight, which was recovered due to MO administration (Fig. 5E and F). Consistently, the increased lipid droplet in the liver of HFD-fed mice was obviously blocked in that of MO-administered mice (Fig. 5G), which was in agreement with hepatic steatosis score (Fig. 5H). Thus, the adipogenic transcription factors were further determined. Mice fed HFD had higher hepatic expression of PPAR $\gamma$ , SREBP1, and C/EBP $\alpha$  than the ND group, but MO-administered group showed remarkably lower PPAR $\gamma$ , SREBP1, and C/EBP $\alpha$  protein expression than the HFD group (Fig. 5I).

## 3. Discussion

Currently available anti-obesity drugs are Phentermine, Orlistat, Lorcaserin, Phentermine-topiramate, Naltrexone-bupropion, and Liraglutide. Orlistat is pancreatic and gastric lipase inhibitors and Liraglutide is GLP-1 receptor agonist. Phentermine, Lorcaserin, Phentermine-topiramate, and Naltrexone-bupropion act on brain, through sympathomimetic, 5-HT<sub>2C</sub> receptor, GABA receptor, and opioid receptor, respectively. These drugs are not widely prescribed and these low rates of prescription might be the result of a long history of adverse events associated with older drugs [13]. In our study, MO-treated group had higher improvement effect on adipogenic factors (PPAR $\gamma$ , SREBP1, and C/EBP $\alpha$ ), p-AMPK, and SIRT1 in adipose tissue than the Orlistat-treated group, showing that MO is not only more effective than Orlistat, but also exhibits anti-obesity effects with a mechanism different from Orlistat. Herbal preparations containing MO cortex are typically used as decoctions with intakes ranging from 3 to 10 g per person. Various Magnolia bark extracts can also be found in the marketplace as ingredients of both dietary supplements, typical recommended use levels ranging from 200 to 800 mg/d per person, and cosmetic product. Animal studies exhibit that magnolia bark and its extracts are of low oral toxicity with an oral LD<sub>50</sub> value > 50 g/kg body weight [14]. Previously it has reported for MO to ameliorate kidney damage in a HFD-induced obese mouse model [15]. Additionally, MO has found to have regulatory effects on obesity-associated lipid accumulation, inflammation, oxidative stress, and apoptosis in the heart of HFD-fed mice [16]. Thus, these evidences support the safety of MO as dietary supplementation against weight control.

Several studies raised the possibility that MO might have anti-obesity activity. Herbal preparation containing MO resulted in a significant decrease in body weight gain, dyslipidemia, and hepatic steatosis [17]. Honokiol alleviated obesity through inhibition of adipogenesis and promotion of white adipose tissue browning in HFD-fed C57BL/6 mice [18]. Magnolol has reported to could alleviate insulin resistance, improve glucose and lipid metabolism dysfunction by lowering free fatty acid level [19]. Our UPLC/MS analysis demonstrated that MO contained Honokiol and Magnolol (Fig. 1). Furthermore, we have conducted the comparative study on anti-obesity effects of MO and the two compounds in 3T3-L1 adipocytes, and our data was consistent with the previous studies showing that Magnolol enhances adipocyte differentiation [20] and Honokiol does not induce adipogenic differentiation *in vitro* [21]. Our result showed that MO has a significant anti-adipogenic effect compared to Magnolol and Honokiol in 3T3-L1 adipocytes, but both MO and the two compounds reduce lipid accumulation in HFD-induced mice model; therefore, it cannot be excluded that they may be the main compounds of the MO in treatment of obesity. This difference supports the need for comparative study of MO and two compounds in *in vivo* model, and further study should be analyzed *in vivo* to reveal the main bioactive compound of MO in treatment of obesity.

Predictably, we found that MO administration for 8 weeks significantly decreased the body weight gain in HFD-fed obese mice. In addition, MO administration did not affect food and energy intake compared to the HFD group; it is consistent with previous data, which showed that, mice given a gavage of 10 mg/kg MO had no significant effects in HFD-induced energy intake changes [16]. Furthermore, MO-administered group had a significantly lower food efficiency ratio than the HFD group, indicating a reduced relative

ability of a food source to contribute to weight gain. However, Weixia Sun et al. have reported that MO treatment slightly increased the body weight between 8 and 21 weeks in HFD-fed C57BL/6J mice, despite of no changes in food intake [16]. This discrepancy is probably explained by the different administration dosage; while previous study has used 10 mg/kg MO, present study used 50 mg/kg of MO. Additional studies are needed to find out the two faces of MO on weight gain.

There has been postulated to correlate in obesity-related metabolic dysfunction and defective fatty acid oxidation, due to evidence that fatty acid oxidation capacity is decreased in obese humans and rodents; therefore, strategies that concentrate on enhancing fatty acid oxidation have been developed to prevent obesity with positive results [22]. Acox is an enzyme responsible for the fatty acid oxidation, which initiates the process of long-chain fatty acid oxidation [23]. PPAR $\alpha$  promotes the target genes involved in fatty acid oxidation [23]. Here, one of the major modulators of this system is the AMPK; generally, AMPK blocks ATP-consuming processes, whereas activating catabolic pathways; active AMPK inhibits the expression of fatty acid synthase, resulting in decrease of the flux of substrates in the fatty acid anabolic pathway [24]. The regulation of AMPK by members of the sirtuin family has been reported; the AMPK activity contributes to an increase in NAD<sup>+</sup> levels, thus stimulating deacetylation/activation of other SIRT1 targets associated with fatty acid oxidation, including PGC-1 $\alpha$  [24]. Previous study was reported that Magnolol prevented IL-1B-induced mitochondrial dysfunction, inflammation, and oxidative stress through SIRT1 signaling [9]. It is also involved in promotion of  $\beta$ -cell survival and functions by increasing the expression of SIRT1 [10]. In addition, Bin Zhang et al. have reported that Honokiol ameliorated diabetic myocardial ischemia/reperfusion injury and SIRT1 played a pivotal role in this process [11]. Hong Ye et al. have reported that Honokiol regulates endoplasmic reticulum stress by promoting the activation of the SIRT1-mediated protein kinase B pathway [12]. In agreement with these previous studies, we found that MO administration significantly reversed the lipogenesis and fatty acid oxidation genes by increasing the SIRT1 expression in white adipose tissue, and it also inhibited the adipogenesis via up-regulation of SIRT1 in 3T3-L1 adipocytes. However, to evaluate whether MO directly regulates SIRT1 in adipocytes, further study should be analyzed.

When the adipose tissue cannot store immoderate fat, lipids accumulate inappropriately in other tissue including liver. The HFD-induced hepatic steatosis was recovered after MO administration by inhibiting the protein expression of PPAR $\gamma$ , SREBP1, and C/EBP $\alpha$ , which was congruent with the previous studies showing that MO prevented alcoholic fatty liver [25], HFD-induced liver damage [26], and reversed free fatty acid-induced lipogenesis in hepatocytes [27]. These findings suggest that MO may protect obesity-induced non-alcoholic fatty liver disease.

In conclusion, we report that MO inhibits the expression of key adipogenic transcription factors (PPAR $\gamma$ , SREBP1, and C/EBP $\alpha$ ) and increases the expression of p-AMPK and SIRT1 in 3T3-L1 adipocytes and adipose tissue of HFD-induced obese mice, leading to alleviation of weight gain. Furthermore, it inhibits the expression of these adipogenic transcription factors in liver tissue, improving hepatic steatosis. Our results suggest that MO could be important candidate for treating weight gain and obesity-induced hepatic steatosis.

## 4. Methods

### 4.1. Chemicals and reagents

Dulbecco's modified Eagle's medium (DMEM), bovine serum (BS), fetal bovine serum, and antibiotic-antimycotic (ABAM) were obtained from Life Technologies, Inc. (Grand Island, NY, USA). 3-Isobutyl-1-methylxanthine (IBMX), dexamethasone (DEX), insulin, and Oil Red O powder were purchased from Sigma-Aldrich Co. LLC (St. Louis, MO, USA). A 45% HFD was acquired from Research Diets (New Brunswick, NJ, USA). Antibodies against PPAR $\gamma$  (cat. No. sc-7273), C/EBP $\alpha$  (cat. No. sc-9314), SREBP1 (cat. No. sc-13551), SIRT1 (cat. No. sc-74465), and  $\beta$ -actin (cat. No. sc-81178) were purchased from Santa Cruz Biotechnology, Inc. (Dallas, TX, USA), and p-AMPK (cat. No. #2531) and AMPK (cat. No. #2532) were purchased from Cell Signaling Technology, Inc. (Danvers, MA, USA). Horseradish peroxidase conjugated secondary antibodies were obtained from Jackson ImmunoResearch Laboratories, Inc. (West Grove, PA, USA).

### 4.2. Preparation of MO

MO (*Magnolia officinalis* Rehder & E. Wilson; record 117741) acquired from Nanum Pharmaceutical Company (Seoul, Republic of Korea). Extraction yield of herbs was performed as previously described [28]. Herbs were extracted in water at 99 °C for 3 h. The extract was then freeze-dried and the yield was calculated at 25%. The powder was dissolved in distilled water for subsequent experimentation, and residual powder was stored at -20 °C.

### 4.3. LC/MS

The standard of Honokiol and Magnolol were purchased from Sigma-Aldrich Co. LLC (St. Louis, MO, USA). The water extract of MO and two standards were dissolved in methanol. Thereafter, ultra-performance liquid chromatography was performed on the ACQUITY UPLC system (Waters, MA, USA) with an ACQUITY binary solvent manager pump (ACQ-BSM), a ACQUITY PDA detector (ACQ-PDA) and Waters micromass ZQ spectrometer (Waters) coupled with an electrospray ionization (ESI) interface and an ion trap mass analyzer. The extract and two standards were analyzed under the following conditions: column, ACQUITY UPLC BEH Shield RP18 (2.1  $\times$  100 mm, 1.7  $\mu$ m; USA); mobile phase, distilled water (solvent system A), and acetonitrile (CH<sub>3</sub>CN, solvent system B) in a gradient mode (B from 10 to 100 % in 15 min); sample injection volume, 5  $\mu$ L; flow rate, 0.3 mL/min; column temperature, 40 °C, UV wavelength, 289 nm. The conditions of MS analysis in the negative ion mode were as follows: capillary voltages, -3.00 kV; cone voltage, -50 V; extractor

**Table 1**  
Antibodies for Western blotting.

A. Primary antibodies			
Antibody	Dilution	Vendor	Catalog No.
PPAR $\gamma$	1:2000	Santa Cruz Biotechnology	sc-7273
C/EBP $\alpha$	1:2000	Santa Cruz Biotechnology	sc-365318
SREBP1	1:2000	Santa Cruz Biotechnology	sc-13551
AMPK	1:1000	Cell signaling	#2532
p-AMPK	1:1000	Cell signaling	#2535
SIRT1	1:1000	Santa Cruz Biotechnology	sc-74465
$\beta$ -actin	1:2500	Santa Cruz Biotechnology	sc-81178
B. Secondary antibodies			
Antibody	Dilution	Vendor	Catalog No.
Rabbit-anti-mouse HRP Conjugate	1:2500	Jackson ImmunoResearch	315-035-003
Goat-anti-rabbit HRP Conjugate	1:2500	Jackson ImmunoResearch	112-035-003

PPAR $\gamma$ , peroxisome proliferator activated receptor  $\gamma$ ; C/EBP $\alpha$ , CCAAT/enhancer-binding protein  $\alpha$ ; SREBP1, sterol regulatory element binding protein 1; AMPK, AMP-activated kinase; SIRT1, Sirtuin 1.

voltage, - 2 V; RF lens voltage, - 0.2 V; source temperature 120 °C, desolvation temperature 400 °C, gas flow desolvation 600 L/h, gas flow cone 30 L/h.

#### 4.4. Experimental animals

All experimental procedures were approved by the Ethical Committee for Animal Care and Use of Laboratory Animals of Sangji University (reg.no. 2018–28). Briefly, thirty male C57BL/6 N mice ( $20 \pm 2$  g) at 8 weeks of age were used in these animal experiments ( $n = 6$  per group). Mice were housed in a 12 h light/dark cycle,  $22 \pm 2$  °C, and  $55\% \pm 9\%$  humidity. After a week of acclimation, mice were fed either a normal diet (ND) or 45% high-fat diet (HFD) (D-12451, Research Diets (New Brunswick, NJ, USA)). For drug treatment, Orlistat (20 mg/kg) and MO (50 mg/kg) were administered to mice via oral gavage for 8 weeks except weekend. The Orlistat was obtained from Tokyo Chemical Inc. (Tokyo, Japan). Mice had free access to water and diet. Body weight and food intake were monitored weekly. At the end of the experiments, all animals were euthanized by Zoletil 50 (20 mg/kg, i.p.) and cervical dislocation. Liver and adipose tissues were taken and rapidly stored at  $-80$  °C.

#### 4.5. Biochemical analysis

Serum biochemical analysis was performed as previously described [29]. Blood was collected and immediately centrifuged ( $1000 \times g$  for 20 min at 4 °C) to obtain the plasma. The levels of total cholesterol (TC), triglycerides (TG), aspartate aminotransferase (AST), and alanine aminotransferase (ALT), in the plasma were measured using commercial kits (Asan Pharmaceutical. Co. Ltd., Republic of Korea). All biochemical assay was conducted according to the manufacturer's instructions.

#### 4.6. Histological examination

Histological analyses of epididymal white adipose tissue and liver were performed as previously described [29]. Epididymal adipose tissue and liver from representative mice were fixed in 10% formalin, embedded into paraffin and cut into 5  $\mu$ m sections. The sections were then used for hematoxylin/eosin staining. The stained liver sections were observed for examination of lipid droplets. The stained adipose tissue sections were used to measure the size of adipocytes. All observations were performed using an Olympus SZX10 microscope.

#### 4.7. Western blot analysis

Western blot analysis was performed as previously described [30]. The 3T3-L1 adipocytes, epididymal adipose tissue, and liver tissues were homogenized with PRO-PREP<sup>TM</sup> protein extraction solution (Intron Biotechnology, Seoul, Republic of Korea). Equal amounts (15–30  $\mu$ g) of protein sample were separated on a sodium dodecyl sulfate polyacrylamide gel, and then transferred onto a polyvinylidene fluoride membrane. Membranes were incubated overnight with primary antibodies, and then incubated with horseradish peroxidase-conjugated secondary antibody for 2 h. The antibodies are listed in Table 1. The blots were again washed three times with tris buffered saline with tween 20 and then visualized by enhanced chemiluminescence using Amersham<sup>TM</sup> Imager 680 (GE Healthcare Bio-Sciences AB, Sweden).

#### 4.8. Reverse transcription-quantitative polymerase chain reaction (RT-qPCR) analysis

The epididymal white adipose tissue was homogenized and the mRNA levels was conducted using a Step One Plus Real-time PCR

**Table 2**  
Real-Time polymerase chain reaction (PCR) primer sequences.

Gene	Forward (5'–3')	Reverse (3'–5')
<i>FAS</i>	AGGGGTCGACCTGGTCCTCA	GCCATGCCCAGAGGGTGGTT
<i>ChREBP</i>	CACTCAGGAATACAGCGCTAC	ATCTTGGTCTTAGGGTCTTCAGG
<i>Acox</i>	TAACTTCTCACTCGAAGCCA	AGTTCCATGACCCATCTCTGTGTC
<i>PGC1<math>\alpha</math></i>	TATGGAGTGACATAGAGTGTGCT	CCACTTCAATCCACCCAGAAAG
<i>PPAR<math>\alpha</math></i>	CAGGAGAGCAGGGATTGCA	CCTACGCTCAGCCCTCTTCAT
<i>AMPK</i>	GGTGGATTCCAAAAGTGCT	AAGCAGTGCTGGGTCACAAG
<i>SIRT1</i>	TGCCATCATGAAGCCAGAGA	AACATCGCAGTCTCCAAGGA
<i>GAPDH</i>	GACGGCCGCATCTTCTTGT	CACACCGACCTTCACCATTIT

system (Applied Biosystems, Thermo Fisher Scientific, Inc., Waltham, MA, USA) as described [30]. *GAPDH* was used as an internal control. The sequences of the mouse oligonucleotide primers (Bioneer Corporation (Daejeon, Korea)) are shown in Table 2.

#### 4.9. Cell culture and treatment

3T3-L1 preadipocytes were obtained from the American Type Culture Collection (ATCC, Manassas, VA, USA; CL-173) and were cultured in DMEM containing 10% BS, 1% ABAM, 1 g/L HEPES, and 1.5 g/L sodium bicarbonate. The 3T3-L1 adipocytes differentiation was performed as previously described [31]. To stimulate adipocyte differentiation, cells were seeded at a density of  $2 \times 10^5$  per well into 6-well plates to confluence (Day 0). Then, cells were differentiated with MDI medium containing 0.5 mM IBMX, 1  $\mu$ M DEX, and 1  $\mu$ g/mL insulin in culture medium (Day 2). The cells were also differentiated in culture medium containing 1  $\mu$ g/ml insulin (Day 4). The culture medium was changed with 125  $\mu$ g/mL MO, 10  $\mu$ M Magnolol, or 10  $\mu$ M Honokiol every 2 days, until days 6–8. The human hepatoma cell line HepG2 (No. 88065) was obtained from the Korean Cell Line Bank (KCLB, Seoul, Republic of Korea). HepG2 cells were grown in MEM containing 10% FBS and 100 mg/L penicillin under a humidified atmosphere of 5% CO<sub>2</sub> at 37 °C. The cells were seeded at a density of  $2 \times 10^5$  cells per well into 6-well plate and then treated with 1 mM oleic acid (O 7501, Sigma-Aldrich) dissolved in culture medium containing 5% methanol with or without different concentrations of MO for 48 h.

#### 4.10. Cell viability assay

Cell viability was performed as previously described [31]. 3T3-L1 preadipocytes and HepG2 cells were seeded on 96-well plates at density  $1 \times 10^4$  cells per well. The cells were treated with different concentrations of MO for 48 h. The 3-(4,5-dimethylthiazol-2-yl)-2,5-diphenyl tetrazoliumbromide (MTT) solution (5 mg/ml) was treated and the cells were incubated at 37 °C for 4 h. After discarding the supernatant, 100  $\mu$ L of dimethyl sulfoxide was added to dissolve formazan crystals, and the MTT-formazan product was measured using an Epoch® microvolume spectrophotometer (Bio Tek Instruments Inc., Winooski, VT, USA) at 570 nm.

#### 4.11. Oil Red O staining

The Oil Red O staining was performed as previously described [31]. 3T3-L1 preadipocytes and HepG2 cells were cultured with or without differentiation conditions in the presence or absence of indicated concentrations of MO. The cells were washed three times with phosphate-buffered saline (PBS) and fixed with 10% formaldehyde in PBS at 25 °C for 1 h. After fixation, cells were washed three times with distilled water and then stained with Oil Red O working solution (3 mg/ml ORO in 60% isopropanol) at 25 °C for 2 h. Cells were rinsed three times with distilled water and photographed with an Olympus SZX10 microscope (Tokyo, Japan). The Oil Red O dye was dissolved by isopropanol and measured with an Epoch® microvolume spectrophotometer at 520 nm.

#### 4.12. Statistical analysis

Each result is represented as the mean  $\pm$  standard deviation of triplicate experiments. Statistical analysis was performed using SPSS version 19.0 (International Business Machines, Armonk, NY, USA). Statistical significance was determined using analysis of variance and Dunnett's post-hoc test. P-values less than 0.05 were considered statistically significant amongst experimented groups.

#### Ethics statement

All experimental procedures were approved by the Ethical Committee for Animal Care and Use of Laboratory Animals of Sangji University (reg.no. 2018–28).

#### Data Availability statement

Data will be made available on request.

## CRedit authorship contribution statement

**Yea-Jin Park:** Writing – review & editing, Writing – original draft, Data curation, Conceptualization. **Hee-Young Kim:** Investigation. **Tae-Young Gil:** Investigation. **Hyo-Jung Kim:** Investigation. **Jong-Sik Jin:** Investigation, Methodology. **Yun-Yeop Cha:** Project administration, Funding acquisition. **Hyo-Jin An:** Supervision, Project administration.

## Declaration of competing interest

The authors declare that they have no known competing financial interests or personal relationships that could have appeared to influence the work reported in this paper.

## Acknowledgement

This research was supported by National Research Foundation of Korea (NRF), funded by the Ministry of Science, ICT & Future Planning, grant number NRF-2021R1A2C3011862.

## Appendix A. Supplementary data

Supplementary data to this article can be found online at <https://doi.org/10.1016/j.heliyon.2024.e27600>.

## References

- [1] M. Bluher, Metabolically healthy obesity, *Endocr. Rev.* 41 (2020), <https://doi.org/10.1210/edrv/bnaa004>.
- [2] Chen, K. et al. HMGB2 orchestrates mitotic clonal expansion by binding to the promoter of C/EBPbeta to facilitate adipogenesis. *Cell Death Dis.* 12, 666, doi: 10.1038/s41419-021-03959-3(2021).
- [3] Majeed, Y. et al. SIRT1 promotes lipid metabolism and mitochondrial biogenesis in adipocytes and coordinates adipogenesis by targeting key enzymatic pathways. *Sci. Rep.* 11, 8177, doi:10.1038/s41598-021-87759-x(2021).
- [4] R. Nogueiras, et al., Sirtuin 1 and sirtuin 3: physiological modulators of metabolism, *Physiol. Rev.* 92 (2012) 1479–1514, <https://doi.org/10.1152/physrev.00022.2011>.
- [5] S.P. Narula, P.L. Sharma, P.L. Wahi, Antiarrhythmic activity of racemic propranolol and its optical isomers in ouabain-induced cardiac arrhythmias in rhesus monkeys, *Indian J. Med. Res.* 63 (1975) 1705–1711.
- [6] L. Niu, Y. Hou, M. Jiang, G. Bai, The rich pharmacological activities of *Magnolia officinalis* and secondary effects based on significant intestinal contributions, *J. Ethnopharmacol.* 281 (2021) 114524, <https://doi.org/10.1016/j.jep.2021.114524>.
- [7] S. Emerenziani, et al., Role of overweight and obesity in gastrointestinal disease, *Nutrients* 12 (2019), <https://doi.org/10.3390/nu12010111>.
- [8] F. Schifano, et al., Is there a potential of misuse for *Magnolia officinalis* compounds/metabolites? *Hum. Psychopharmacol.* 32 (2017) <https://doi.org/10.1002/hup.2595>.
- [9] Z. Liu, H. Zhang, H. Wang, L. Wei, L. Niu, Magnolol alleviates IL-1beta-induced dysfunction of chondrocytes through repression of SIRT1/AMPK/PGC-1alpha signaling pathway, *J. Interferon Cytokine Res.* 40 (2020) 145–151, <https://doi.org/10.1089/jir.2019.0139>.
- [10] K.S. Suh, S. Chon, W.W. Jung, E.M. Choi, Magnolol protects pancreatic beta-cells against methylglyoxal-induced cellular dysfunction, *Chem. Biol. Interact.* 277 (2017) 101–109, <https://doi.org/10.1016/j.cbi.2017.09.014>.
- [11] B. Zhang, et al., Honokiol ameliorates myocardial ischemia/reperfusion injury in type 1 diabetic rats by reducing oxidative stress and apoptosis through activating the SIRT1-nrf2 signaling pathway, *Oxid. Med. Cell. Longev.* (2018) 3159801, <https://doi.org/10.1155/2018/3159801>, 2018.
- [12] H. Ye, Y. Meng, Honokiol regulates endoplasmic reticulum stress by promoting the activation of the sirtuin 1-mediated protein kinase B pathway and ameliorates high glucose/high fat-induced dysfunction in human umbilical vein endothelial cells, *Endocr. J.* 68 (2021) 981–992, <https://doi.org/10.1507/endocrj.EJ20-0747>.
- [13] D.H. Bessesen, L.F. Van Gaal, Progress and challenges in anti-obesity pharmacotherapy, *Lancet Diabetes Endocrinol.* 6 (2018) 237–248, [https://doi.org/10.1016/S2213-8587\(17\)30236-X](https://doi.org/10.1016/S2213-8587(17)30236-X).
- [14] N. Li, et al., Evaluation of the in vitro and in vivo genotoxicity of magnolia bark extract, *Regul. Toxicol. Pharmacol.* : RTP (Regul. Toxicol. Pharmacol.) 49 (2007) 154–159, <https://doi.org/10.1016/j.yrtph.2007.06.005>.
- [15] W. Cui, et al., Magnolia extract (BL153) ameliorates kidney damage in a high fat diet-induced obesity mouse model, *Oxid. Med. Cell. Longev.* 2013 (2013) 367040, <https://doi.org/10.1155/2013/367040>.
- [16] W. Sun, et al., Magnolia extract (BL153) protection of heart from lipid accumulation caused cardiac oxidative damage, inflammation, and cell death in high-fat diet fed mice, *Oxid. Med. Cell. Longev.* 2014 (2014) 205849, <https://doi.org/10.1155/2014/205849>.
- [17] M. Yimam, et al., UP601, a standardized botanical composition composed of *Morus alba*, *Yerba mate* and *Magnolia officinalis* for weight loss, *BMC Compl. Alternative Med.* 17 (2017) 114, <https://doi.org/10.1186/s12906-017-1627-1>.
- [18] Y. Ding, et al., Honokiol alleviates high-fat diet-induced obesity of mice by inhibiting adipogenesis and promoting white adipose tissue browning, *Animals (Basel)* 11 (2021), <https://doi.org/10.3390/ani11061493>.
- [19] W.L. Zhang, L. Zhu, J.G. Jiang, Active ingredients from natural botanicals in the treatment of obesity, *Obes. Rev. : an official journal of the International Association for the Study of Obesity* 15 (2014) 957–967, <https://doi.org/10.1111/obr.12228>.
- [20] S.S. Choi, et al., Magnolol enhances adipocyte differentiation and glucose uptake in 3T3-L1 cells, *Life Sci.* 84 (2009) 908–914, <https://doi.org/10.1016/j.lfs.2009.04.001>.
- [21] A.G. Atanasov, et al., Honokiol: a non-adipogenic PPARgamma agonist from nature, *Biochim. Biophys. Acta* 1830 (2013) 4813–4819, <https://doi.org/10.1016/j.bbagen.2013.06.021>.
- [22] R. Fucho, N. Casals, D. Serra, L. Herrero, Ceramides and mitochondrial fatty acid oxidation in obesity, *FASEB J* 31 (2017) 1263–1272, <https://doi.org/10.1096/fj.201601156R>.
- [23] Y.T. Yeh, Y.Y. Cho, S.C. Hsieh, A.N. Chiang, Chinese olive extract ameliorates hepatic lipid accumulation in vitro and in vivo by regulating lipid metabolism, *Sci. Rep.* 8 (2018) 1057, <https://doi.org/10.1038/s41598-018-19553-1>.
- [24] D. Serra, P. Mera, M.I. Malandrino, J.F. Mir, L. Herrero, Mitochondrial fatty acid oxidation in obesity, *Antioxidants Redox Signal.* 19 (2013) 269–284, <https://doi.org/10.1089/ars.2012.4875>.

- [25] H.Q. Yin, et al., Magnolia officinalis reverses alcoholic fatty liver by inhibiting the maturation of sterol regulatory element-binding protein-1c, *J. Pharmacol. Sci.* 109 (2009) 486–495, <https://doi.org/10.1254/jphs.08182fp>.
- [26] J. Wang, et al., BL153 partially prevents high-fat diet induced liver damage probably via inhibition of lipid accumulation, inflammation, and oxidative stress, *Oxid. Med. Cell. Longev.* 2014 (2014) 674690, <https://doi.org/10.1155/2014/674690>.
- [27] M.S. Seo, et al., Magnolia officinalis attenuates free fatty acid-induced lipogenesis via AMPK phosphorylation in hepatocytes, *J. Ethnopharmacol.* 157 (2014) 140–148, <https://doi.org/10.1016/j.jep.2014.09.031>.
- [28] I.S. Kim, M.R. Yang, O.H. Lee, S.N. Kang, Antioxidant activities of hot water extracts from various spices, *Int. J. Mol. Sci.* 12 (2011) 4120–4131, <https://doi.org/10.3390/ijms12064120>.
- [29] A. Ansari, et al., CST, an herbal formula, exerts anti-obesity effects through brain-gut-adipose tissue Axis modulation in high-fat diet fed mice, *Molecules* 21 (2016), <https://doi.org/10.3390/molecules21111522>.
- [30] Y.J. Park, G.S. Lee, S.Y. Cheon, Y.Y. Cha, H.J. An, The anti-obesity effects of Tongbi-san in a high-fat diet-induced obese mouse model, *BMC Compl. Alternative Med.* 19 (2019) 1, <https://doi.org/10.1186/s12906-018-2420-5>.
- [31] Y.J. Park, D.W. Seo, J.Y. Ju, Y.Y. Cha, H.J. An, The antiobesity effects of buginawa in 3T3-L1 preadipocytes and in a mouse model of high-fat diet-induced obesity, *BioMed Res. Int.* 2019 (2019) 3101987, <https://doi.org/10.1155/2019/3101987>.